

A Review of Engineering Approaches for Lymphedema Detection

Karina Rincon, Pratikkumar Shah, Jessica Ramella-Roman, and Shekhar Bhansali, *Member, IEEE*

(Methodological Review)

Abstract—Edema is a condition characterized by excessive swelling of a tissue due to an abnormal accumulation of interstitial fluid in the subcutaneous tissue. More specifically, disruption of the lymphatic system causes what is known as lymphedema. This condition is commonly seen in breast cancer survivors postradiotherapy treatment, chemotherapy, and surgeries; this population has shown high risk of developing lymphedema in the limbs. Throughout the years, several techniques have been developed and implemented for the detection and measurement of lymphedema, including techniques to measure the diseased limb volume, electrical techniques to measure the water content in tissues, and optical techniques to measure either tissue absorbance or limb volume. However, there is still no method that allows for continuous monitoring of the disease and provides a better understanding of its progression. This study describes the different approaches that have been used and that could be used for lymphedema measurement.

Index Terms—Bioelectrical impedance, blood flow, lymphedema, optical spectroscopy, water content.

I. INTRODUCTION

THE SKIN is the largest organ in the body that acts as the first line of defense against environmental factors. Its importance is vital as it prevents pathogens from entering the body, regulates body temperature, and prevents the body from losing water. The skin has different layers; the stratum corneum, which is its outermost layer, has a thickness that ranges between 8 and 20 μm , being much thicker on the soles of the feet and the palms of the hands [1], [2]. The stratum corneum forms part of the epidermis, and it does not have a planar and rigid structure. The dermis, which is underneath the epidermis, is mainly composed of capillaries and lymph vessels. Skin thickness varies largely from organ to organ. The epidermis is only 0.05 mm thick on the eyelids, whereas 1.5 mm thick on palms and soles of the feet. Similarly, the thickness of the dermis varies from 1.5 to 4 mm [3].

Manuscript received November 23, 2015; revised April 10, 2016; accepted May 23, 2016. Date of publication June 20, 2016; date of current version September 16, 2016. This work was supported by the National Science Foundation under NSF I Corp., Grant 1444327 and the Florida Georgia Louis Stoke Alliance for Minority Participation under NSF Grant 1301998.

K. Rincon, P. Shah, and S. Bhansali are with the Department of Electrical and Computer Engineering, Florida International University, Miami, FL 33174 USA (e-mail: krinc005@fiu.edu; pshah003@fiu.edu; sbhansa@fiu.edu).

J. Ramella-Roman is with the Department of Biomedical Engineering, Florida International University, Miami, FL 33174 USA (e-mail: jramella@fiu.edu).

Digital Object Identifier 10.1109/RBME.2016.2582178

Normally, in the body, the hydrostatic pressure of a capillary is about 35 mmHg in the arteriole and 18 mmHg in the venule [4]. Additionally, the normal osmotic pressure of a capillary is 25 mmHg for both arterioles and venules [4]. Disruption of these pressures will alter the normal osmotic balance, which consequently causes edema.

Edema is a medical condition characterized by subdermal accumulation of fluids. Although edema can occur anywhere in the body, it is most commonly seen in the ankles, feet, and legs. Common causes of edema include increased hydrostatic pressure, decreased plasma proteins, increased capillary permeability, and blockage of the lymphatic system.

The lymphatic system is composed of a network of lymph vessels (some of which are found in the dermis), tissues, and organs that transport lymph fluid throughout the whole body. It is the system that prepares the body when it is time to fight an infection or disease.

Lymphedema occurs due to a disruption of the lymphatic system, causing an abnormal accumulation of fluid in the subcutaneous tissue (hypodermis) [5]. The more the fluid accumulates, the more the tissue swells, resulting in decreased blood flow in the blood vessels of the dermis. This condition is commonly seen in breast cancer survivors who have had cancer surgery and/or have been exposed to cancer treatments such as chemotherapy and radiation.

Throughout the years, there have been several efforts to develop an approach for measuring and detecting lymphedema. Researchers have used different techniques to do this, from simple measures of volumes like water displacement, to bioelectrical impedance and optical spectroscopy. However, a method that provides enough insight of this disease and its progression still remains a clinical need [6].

II. LYMPHEDEMA

The lymphatic system is responsible for the drainage of materials including proteins and cells (macrophages, lymphocytes, and even malignant cells) that are unable to return to the bloodstream [7]. There are two types of lymphatics, noncontractile initial lymphatics or capillaries, which are concerned with absorption and transportation of fluid and proteins from the interstitial space to the second type of lymphatics, commonly known as larger contractile vessels or collectors. These pump lymph toward the lymph nodes in a unidirectional flow controlled with secondary lymphatic valves [7], [8].

Some factors that improve the absorption and transportation of lymph within vessels include skeletal muscle contractions,



Fig. 1. Individual with acute lymphedema of the right leg (left) versus a healthy individual (right) made from “Make Human” [10].

which cause tissue deformation, pulsation of neighboring arteries, as well as local massage [5]. The lymphatic system is also important for cellular immunity as it directs the antigen presenting cells to the lymph nodes in response to an infection [9]. Therefore, proper function of the lymphatic system is critical for a healthy individual.

When the lymphatic system is working properly, lymph is transported throughout the body and then, it is delivered back to the bloodstream. However, when the lymphatic system is blocked or damaged, the fluid is not drained from the tissues [11]. As a consequence, an abnormal accumulation of extracellular fluid occurs, leading to excessive swelling of the tissue (see Fig. 1). As the fluid accumulation increases and the tissue swells, the pressure build up in the affected limb causes a decrease in blood flow. In order to detect lymphedema, the amount of fluid accumulated must be higher than 100%; otherwise, it cannot be clinically detectable [11].

It is important not to confuse lymphedema with other types of edema. For instance, in dermal edema, the interfollicular dermis is expanded, and in deep subcutaneous edema, the skin will present pitting [12], [13]. The majority of edemas occur when the capillary filtration rate exceeds lymph drainage rate [14], [15]. This causes the drainage of lymph fluid to be overwhelmed, resulting in failure of the lymphatic system [11]–[14]. However, the underlying cause of lymphedema is the malfunction of the drainage of lymph fluid when the transport of lymph is less than normal [11].

When lymphedema starts to develop, it is possible to observe the swelling in the tissue which becomes soft and easy to pit. Nevertheless, as the condition progresses and the swelling increases, the subcutaneous tissue becomes harder and firmer because of fibrosis and fat deposition, and the tissue becomes harder to pit. The Stemmer’s sign (i.e., when the skin fold at the base of a second toe is too thick to pinch) is usually positive in patients that have had lymphedema of the legs for a certain time [16]. Furthermore, when a patient has chronic lymphedema, some of the most prominent skin changes that arise as the condition progresses include papillomatosis, lymphangiectasia, and hyperkeratosis [17]–[19].

In order to understand lymphedema better, it is important to know where the excess lymph is produced and the location

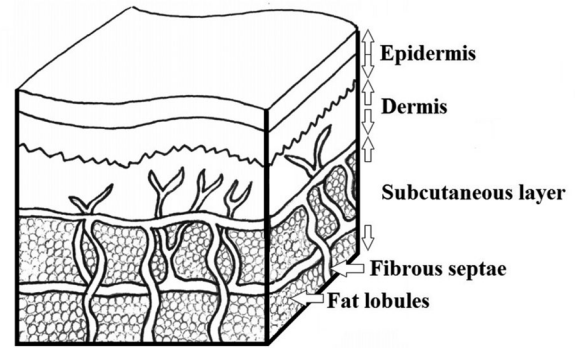


Fig. 2. Skin anatomy image. Fluid accumulation in lymphedema occurs between the fat lobules and the fibrous septa adapted from [21].

where it accumulates as tissue fluid. Olszewski *et al.* [20] found that lymph was present in the subepidermal lymphatics only, whereas the bulk of stagnant tissue fluid was accumulated in the subcutis or hypodermis between fat lobules and fibrous septa (see Fig. 2), but also underneath and above the muscular fascia.

There are two types of lymphedema: primary or secondary. Primary lymphedema occurs when a person is born with an abnormal lymphatic system. This type of lymphedema can be further classified as congenital, praecox, or tarda, depending on the age of the onset. Congenital lymphedema is evident from the birth, more common in females, and accounts for about 10% to 25% of all primary lymphedema cases [7], [22]–[24]. Lymphedema praecox, accounts for 65% to 80% of all primary lymphedema cases; it becomes apparent between birth and before the age of 35 with symptoms most often developed during puberty [7], [24]–[26]. Lastly, those who develop lymphedema after 35 years old, only account for about 10% of all primary lymphedema cases, and this type is known as lymphedema tarda [7], [24], [27]. Additionally, primary lymphedema can also be classified as familial when the condition is inherited and sporadic when it is not inherited. Familial causes are less common than sporadic, affecting only 5%–10% of primary lymphedema cases [28].

Secondary lymphedema is caused when the lymphatic system is blocked or damaged due to certain factors, such as radiation, burns, tumors, infections, and/or trauma [29], [30]. In the United States, the most common cause of secondary lymphedema is breast cancer surgery combined with radiation therapy [31]–[33]. Generally, breast cancer survivors tend to develop unilateral lymphedema of an arm [34]–[36]. However, worldwide, filariasis (lymph node infestation by a parasite) is the most common cause of secondary lymphedema, and it is widely known as the most common cause of permanent disability in the world [37], [38]. Mosquitoes are responsible for transmitting the larvae that travel to the lymphatics, eventually hatching into worms that disrupt the lymphatic system causing lymphedema. Additionally, the cause of lymphedema development in patients with recurrent infections may be attributed to lymphatic damage due to repeated episodes of cellulitis [39], [40]. Although it is complicated to demonstrate that lymphedema can be caused by infection, recurrent infection may lead to progressive damage of the lymphatic system through lymphangitis and lymphangiothrombosis, which would eventually cause lymphedema [41].

There are up to ten million Americans and hundreds of millions worldwide affected by lymphedema and lymphatic diseases [42]. Currently, there is no technology that offers patients a complete understanding of what actions may aggravate their conditions or that aids in properly managing lymphedema. For instance, would certain movements worsen the condition? How much fluid is accumulated in the swollen tissue? Can the progression of the disease be monitored continuously and in real time? In addition, patients with lymphedema are at high risk of infection because of their compromised lymphatic system.

III. METHODS FOR LYMPHEDEMA DETECTION AND LIMB VOLUME MEASUREMENT

A. Measures of Volume

Measures of volume are techniques that can be easily implemented to detect lymphedema and estimate how much water is being retained in the affected tissue.

1) Water Displacement Measurement: Water displacement has been the long used “gold standard” for lymphedema detection throughout the years. It allows assessing limb volume in a very simple way. However, this technique is rarely used nowadays because of the obvious inconvenience that it presents for the patients. The gold standard consists of measuring the body part by submerging it in a large cylindrical container full of water. Then, the displaced water is measured, providing an estimate of the body part volume [43], [44]. This approach cannot provide accurate information about the exact part/location of a swollen area on the limb. In addition to being inconvenient for patients, this technique is laborious and difficult to use in a clinical setting due to water spillage [45].

2) Tape Measurements: Another common type of a measure of volume in lymphedema patients is tape measurements. In this technique, measurements can be gathered at defined intervals using a tape meter. The collected values can then be used with geometric formulas, in order to calculate the total volume [44], [45]. Although this is a widely used approach, the measurement precision is user dependent [45], [46].

3) Disk Model Method: This common technique consists of dividing the limb into ten disks. Each of these disks is given a size of 5 cm. The next step is to calculate the volume of each of the ten disks and add them. In the arm, the measurements are usually collected at the hand, at the wrist, and below and above the lateral epicondyle [47]. This technique may be easy, inexpensive, and reliable. However, when it comes to limb circumference measurements, it is not possible to obtain an accurate estimate of the hand’s volume because of its asymmetrical shape [46].

4) Frustrum Method (Sitzia’s Method): This technique consists in implementing surface circumference measurements at 4- or 8-cm intervals, along with a mathematical formula (1) derived from a frustrum’s formula, which allows determining the volume of the arm

$$V = \frac{L}{4\pi} (c_1c_2 + c_2c_3 + c_3c_4 + \dots + c_{13}c_{14}) \quad (1)$$

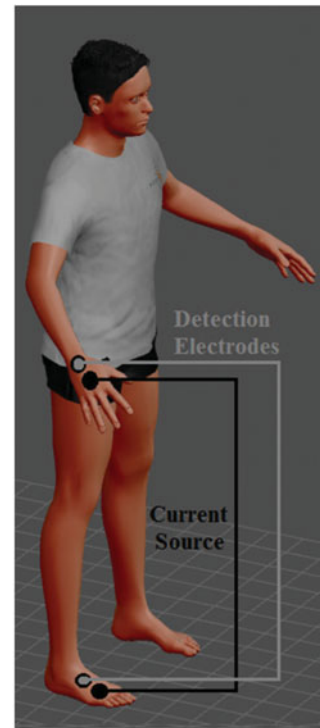


Fig. 3. Standard placement of electrodes on hand and wrist and foot and ankle for the four-electrode concept of bioelectrical impedance [10].

where L is the length of the interval (4 or 8 cm) and c is the circumference of the arm [45], [48].

This method is inexpensive, feasible, and hardly inconvenient for the patient, nevertheless accuracy and precision of the measurement is an issue, just like for the previously described methodologies [45], [48].

B. Electrical Techniques

The study of electrical properties of a tissue dates back to 1786, when Luigi Galvani, an Italian scientist, studied electricity in frog legs [49]. In 1963, Thomasett was the first to demonstrate that an estimate of total body water (TBW) could be obtained when measuring body impedance [50]. He achieved this impedance measurement by inserting two needles subcutaneously.

A four-electrode concept was introduced in 1970s, when Hofer and Nyboer measured the electrical properties of tissues correlating body impedance and the body water content, using dilution techniques as [51]. In general terms, the simplest electrical technique is a noninvasive procedure that consists on placing two electrodes on the right hand and two electrodes on the right foot of a test subject (see Fig. 3) sending a small electrical current throughout the body. Depending on the amount of water in the body, current flow will be affected, and measurements of resistance to the current flow are then possible [52]. This simple technique, known as bioelectrical impedance, provides a good estimate of how much water is in the body, which also allows for calculation of the amount of body fat.

Tissues with high conductivity will contain large quantities of electrolytes and fluids, which allow the current to flow without much resistance, whereas tissues with low conductivity, such as fat and bones, will generate high resistance to the flowing current [52].

For many years, alternating current of 800 μA and a frequency of 50 kHz were used for applications related to measuring impedance in the body [53]. More recently, researchers have been focusing on developing regression models that allow scientists to make better predictions of body composition, including body water [53].

The techniques used for measuring TBW can be either direct or indirect. The direct methods include measuring body water by radioactive isotope dilutions and heavy water dilutions including deuterium oxide [54]. A commonly used formula for calculating the TBW when using the method of deuterium oxide is shown as

$$\text{TBW (L)} = \frac{(D_2O \text{ dose given} - D_2O \text{ in urine})}{4 - h \text{ plasma } D_2O} \quad (2)$$

where the body water is calculated using the retained deuterium oxide dose and the 4- h plasma deuterium oxide concentration [55].

These types of dilution measurements are considered as the gold standard when it comes to measuring body water. Direct measurements are said to be very accurate because they are actual measures of body water. Nevertheless, the majority of direct methods require either ingestion or intravenous administration of these radioactive isotopes. Furthermore, the techniques are time consuming, require careful blood sample analysis, and cannot be repeated over short periods of time [54].

Indirect methods used for estimating TBW include measuring the volume of plasma, the osmolality of urine, and/or analyzing the color of urine. Although, these methods offer an easy and quick assessment of the hydration status of an individual, they are not considered to be very accurate. For instance, plasma volume is only affected by hypohydration after more than 3% of body weight has been lost as water [56]. Additionally, the color and osmolality of urine can be altered by factors other than hydration, such as diseases, medical treatments, and/or foods, which makes these unreliable methods for assessing TBW of an individual.

Despite endless efforts throughout the years, there is still no method that offers 100% accuracy when it comes to measuring body water. Nevertheless, indirect techniques, such as bioelectrical impedance, may present a higher degree of accuracy when it comes to estimating water content in the body, as it has been proven to have a margin of error of approximately 3% [57]. Since bioelectrical impedance allows for measuring water content in the body, it has been used in a few studies for the purpose of estimating the amount of water in patients with lymphedema. Below we will discuss some of these techniques.

1) Single-Frequency Bioelectrical Impedance Analysis (SF-BIA): SF-BIA is a technique that falls under the category of indirect measurements and that appears to provide relatively high accuracy in the assessment of body water content. SF-BIA is usually performed using a single

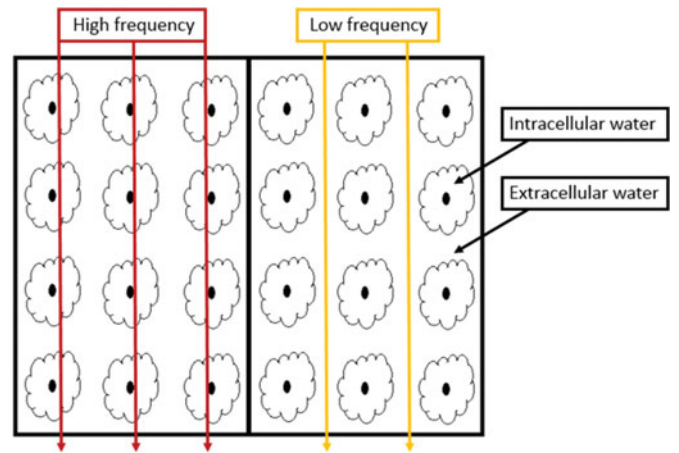


Fig. 4. Current path depending on the frequency applied (adapted from [58], [59]).

frequency of 50 kHz, allowing the current to pass through both the extracellular and intracellular fluids [52]. This technique relies on equations and algorithms that are used to predict and calculate the amounts of water, based on the measured impedance.

Additionally, the single frequency current that is sent throughout the body using electrodes should be a low-level alternating current ($\sim 800 \mu\text{A}$). The electrodes are sometimes used in the configuration depicted in Fig. 4. One of the most widely known formulas for estimating TBW is shown in (3), which was established by Lukaski and Bolonchuk in 1988 [55] and is given by

$$\text{TBW} = 0.372 \left(\frac{S^2}{R} \right) + 3.05 (G) + 0.142 (W) - 0.069 (\text{Age}) \quad (3)$$

where S is the stature, R is the measured skin resistance, G is the gender (0 for females and 1 for males), and W is the weight.

Another slight variation of Lukaski and Bolonchuk's formula [55] obtained from a regression model is given by

$$\text{TBW} = 0.377 \left(\frac{S^2}{R} \right) + 0.14 (W) - 0.08 (\text{Age}) + 2.9 (G) + 4.65. \quad (4)$$

Even though the findings based on the regression model seem encouraging, they are far from conclusive [55]. It is critical to emphasize that this regression equations were developed for healthy individuals, so further research and testing must be done, in order to validate this approach in people who have altered fluid status due to a disease or medical condition.

A study conducted by Kushner and Schoeller, which aimed to measure TBW using bioelectrical impedance plethysmography [60], hypothesized that the lean tissues are mostly composed of water, whereas fat tissue behaves as an insulator, resisting the flow of current. At low frequencies ($f < 50 \text{ kHz}$), the current is conducted by extracellular water (ECW) because the cell walls and the tissue interfaces act as capacitors [53], as seen in Fig. 4. On the other hand, at higher frequencies ($f > 50 \text{ kHz}$),

TABLE I
GROUP MULTIPLE-REGRESSION EQUATIONS FOR PREDICTING TBW IN 40 PARTICIPANTS ADAPTED FROM [60]

BIA-calculate group and sex-specific equations for all 40 subjects (part I)					
Subjects	n	Equation	R	SEE(L) [*]	TE(L) [†]
Males and females	40	(1) (D ₂ O)-TBW = 0.5561 (Ht ² / R) + 0.0955 (Wt) + 1.726	0.986	1.748	1.662
Males	20	(2) (D ₂ O)-TBW = 0.396 (Ht ² / R) + 0.143 (Wt) + 8.399	0.988	1.658	1.509
Females	20	(3) (D ₂ O)-TBW = 0.382 (Ht ² / R) + 0.105 (Wt) + 8.315	0.975	0.884	0.815

*SEE = Standard error of estimate.
†TE = Total error = sqrt [sum(predicted – measured)²/ n].

the current is capable of penetrating extra- and intracellular fluids [60], as shown in Fig. 4. Kushner and Shoeller as well as Lukaski and Bolonchuk used a general formula, shown in (5), to determine the amount of water in the body, where V is the volume of the lean compartment, p is the specific resistivity of the lean tissue, L is the length of the lean compartment, and R is the resistance used to approximate the impedance of the lean tissue, since the reactance can be considered to be a negligible value [52], [60]. This formula assumes that the impedance of a geometrical system is related to the length of the conductor and its configuration [52], [60]

$$V = p \frac{L^2}{R}. \quad (5)$$

Kushner and Shoeller came up with the equations given in Table I, which are based on the measured resistance to estimate the TBW of each individual.

This study appears to prove that SF-BIA improves the accuracy of the prediction of TBW by comparing it to deuterium dilution using regression equations [60]. The method was concluded to be noninvasive, simple, and reliable, which makes it easy to use in ambulatory settings [60]. However, the method may not be very accurate and it may not be used in different populations. Therefore, further studies should be conducted to validate this technique.

Additionally, Sergi *et al.* [61] was able to predict ECW using SF-BIA, but instead of gathering data only at 50 kHz, the study collected data after applying a current of 1 kHz and then a current of 50 kHz. This allowed them to estimate the amount of ECW using (6) and (7) [50], where Ht is the height, Wt is the weight, R is the resistance, X is the reactance, Hh is the health, and G is the gender

$$V_{EW1} = -7.24 + 0.34 \left(\frac{Ht^2}{R_1} \right) + 0.06 (Wt) + 2.63 (Hh) + 2.57 (G) \quad (6)$$

$$V_{EW50} = 5.22 + 0.20 \left(\frac{Ht^2}{R_1} \right) + 0.005 \left(\frac{Wt}{X_{c50}} \right) + 0.08 (Wt) + 1.9 (Hh) \quad (7)$$

Gender (G) = 1 for males and 0 for females

Health (Hh) = 1 for healthy, 2 for diseased.

More recent studies have been focused on epidermal electronics and small wearable sensors to measure hydration status in people. For instance, Rogers and his team have been work-

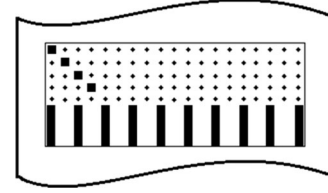


Fig. 5. Miniature stretchable conformal sensor (concept adapted from [62], [63]).

ing on the development of flexible epidermal electronics (see Fig. 5), in which semiconductors are mounted on elastomeric and ultrathin sheets, integrating with the skin through van der Waals forces and with no pressure needed [62], [63]. Their results were compared to those obtained in commercially available moisture meters [62], [63], suggesting that these arrays of miniature sensors that conform to the skin can be developed and implemented for spatial mapping, as well as potentially depth profiling of hydration [62], [63]. This technique could be easily implemented to estimate the amount of water accumulated in a limb using the same or similar principles. To this day though, limited testing has been conducted on wearable sensors, so its reliability and accuracy has not been validated.

Measurement of body water content has become critical over the years, when it comes to assessing health and diseases in individuals. Although it is difficult to measure using direct methods, indirect techniques have provided useful approaches to estimate and predict these values. Furthermore, SF-BIA has not only been used to assess TBW in diseased and healthy individuals, but also have been related to pulsatile blood flow [53]. The fact that bioelectrical impedance provides a way to measure ECW is advantageous when it comes to assessing limb water volume in patients that have been diagnosed with lymphedema, given that this is the type of fluid that accumulates in the affected extremity. However, most of these algorithms have been developed from and for healthy individuals, which is why a single algorithm cannot be suitable for everybody, especially for those with diseases. Implementation of these algorithms in inappropriate populations may result in inaccurate measurements, despite its ease of use and low cost.

2) Multifrequency Bioelectrical Impedance Analysis (MF-BIA): MF-BIA is another common approach used for measuring body composition. This technique consists on collecting impedance measurements at several different

frequencies [64], [65]. The use of different frequencies allows researchers to quantify the amount of ECW at low frequencies, such as 1 or 5 kHz, as well as TBW at higher frequencies, such as 100, 200, or 500 kHz [66], [67]. Based on the measured impedance, linear regression models are implemented in order to estimate water content in the body. For instance, Deurenberg *et al.* [68] used the MF-BIA approach, they used currents of 1, 5, 50, and 100 kHz and proposed (8) and (9) for estimating the volume of ECW, where Z is the impedance

$$V_{\text{ECW}_{1\text{kHz}}} = 2.30 + 0.19528 \left(\frac{Ht^2}{Z_1} \right) + 0.06987 (\text{Wt}) - 0.02 (\text{Age}) \quad (8)$$

$$V_{\text{ECW}_{50\text{kHz}}} = 2.53 + 0.18903 \left(\frac{Ht^2}{Z_0} \right) + 0.06753 (\text{Wt}) - 0.02 (\text{Age}). \quad (9)$$

Additionally, Pichler *et al.* [69] explored the method of bioimpedance spectroscopy (BIS) implementing an ImpediMed device and he established (10) and (11) to estimate the ECW volume in women and men

$$V_{\text{ECW}_{\text{male}}} = 0.11 + 0.11 (\text{Wt}) + 0.24 \left(\frac{Ht^2}{R_{\text{ECW}}} \right) \quad (10)$$

$$V_{\text{ECW}_{\text{female}}} = 0.24 + 0.09 (\text{Wt}) + 0.28 \left(\frac{Ht^2}{R_{\text{ECW}}} \right). \quad (11)$$

Another study performed by Shanholtzer and Patterson consisted in recruiting 100 undergraduate students between the ages of 18 and 30 years of age. The BodyStat Multiscan 5000 multifrequency bioelectrical impedance monitor was used to measure TBW, as well as the distribution of extracellular and intracellular water [70]. Each participant was wearing four electrodes (two on the right hand and two on the right foot). A mild electrical current of 800 μA was sent using a range of frequencies of 5 to 500 kHz through the individual's body and the 5-kHz signal was used to assess ECW, while the 200-kHz signal was used to determine TBW. In this study, four different multiple frequency bioelectrical impedance monitors that are commercially available were compared and it was possible to determine that the Multiscan 5000 had less than 10% error across a range of skin resistance up to 6 k Ω , which was found to be the least amount of error among the four compared machines [70].

The results from this study demonstrated that multifrequency bioelectrical impedance is very reliable when it comes to assessing hydration in healthy individuals, as well as classifying subjects as hyperhydrated or hypohydrated [70]. Hypohydration may be related to medical conditions including diabetes, cardiovascular disease, and hypertension, which means that multifrequency bioelectrical impedance may provide a more reliable technique to determine the hydration status of a person, and, hence, improve patient diagnosis and health care. However, one of the challenges is determining whether it can be possible to detect small changes in hydration status over longer periods of time, i.e., months or years [70], [71].

3) Bioimpedance Spectroscopy: The technique of BIS is a variation of the method of MF-BIA, where a multifre-

quency approach is also used to measure bioimpedance; however, in this case, a range of frequencies from 5 up to 1000 kHz are used. After gathering the multifrequency impedance measurements, based on the Cole–Cole model, the data undergo a nonlinear curve fitting. Then ECW, ICW, and TBW can be calculated by applying the terms from the Cole model to the equations that were derived from the commonly known Hanai mixture theory [72]. In order to utilize BIS, for estimating the volume of body fluid, the first thing that must be done is determining the ECW resistance (R_{ECW}), which is calculated extrapolating to zero and infinite frequencies [73]. Then, the human body is assumed to be composed by five cylinders, corresponding to the four limbs and the trunk, which allows to obtain an approximation of the human body by adding the five cylinders through a dimensionless factor (K_b) [73]. This factor is obtained using the length and perimeters of the trunk and body extremities. A commonly known value for the K_b factor is 4.3, as calculated by Van Loan *et al.* [73], [74] from statistical adult measurements. The general formula for the resistance of the body is given as

$$R = \frac{K_b \rho H^2}{V_b} \quad (12)$$

where V_b is the volume of the body, H is the height, and ρ is the fluid resistivity [73].

Afterward, using Hanai's "mixture" equations from his theory of conductivity, the effect of nonconducting tissue can be calculated with (13), where ρ_a is the apparent resistivity, which takes into account the effect of the nonconducting tissues, and c is the volume fraction [51], [72], [73], which is given by (14):

$$\rho_a = \frac{\rho}{(1-c)^{\frac{3}{2}}} \quad (13)$$

$$c = 1 - \left(\frac{V_{\text{ECW}}}{V_b} \right). \quad (14)$$

The total volume of the body and the apparent resistance are given by (15) and (16), respectively [51]. In addition, because at low frequencies, only ECW is conducting the current, (17)–(20) provide a way to estimate the ECW volume using the apparent resistivity of ECW, the resistance of ECW, and the ECW factor K_{ECW}

$$V_b = \frac{\text{Wt}}{D_b} \quad (15)$$

$$R_a = \frac{K_b \rho H^2}{V_b (1-c)^{\frac{3}{2}}} \quad (16)$$

$$\rho_{a\text{ECW}} = \rho_{\text{ECW}} \left(\frac{V_b}{V_{\text{ECW}}} \right)^{\frac{3}{2}} \quad (17)$$

$$R_{\text{ECW}} = K_b \rho_{\text{ECW}} \left[\frac{\left(\frac{\text{Wt}}{D_b} \right)^{\frac{1}{2}}}{(V_{\text{ECW}})^{\frac{3}{2}}} \right] \quad (18)$$

$$K_{\text{ECW}} = 10^{-2} \left[\frac{K_b \rho_{\text{ECW}}}{\left(D_b^{\frac{1}{2}} \right)} \right]^{\frac{2}{3}} \quad (19)$$

$$V_{ECW} = K_{ECW} \left[\frac{(Ht^2)(Wt)^{\frac{1}{2}}}{R_{ECW}} \right]^{\frac{2}{3}}. \quad (20)$$

The resistivity of the ECW was found to be $42.3 \Omega \cdot \text{cm}$ for women and $40.3 \Omega \cdot \text{cm}$ for men when Hanai [51], [72] performed his calculations, which is very similar to the calculations done by De Lorenzo *et al.* [51], [58], obtaining $39.0 \Omega \cdot \text{cm}$ for women and $40.5 \Omega \cdot \text{cm}$ for men. These two studies gave results that are very close to the resistivity of saline and to the resistivity of ECW composed of plasma and interstitial water, which is about $40 \Omega \cdot \text{cm}$.

Furthermore, ImpediMed has two devices that have already been cleared by the FDA. The first one, Imp SFB7 [69], uses the principles of bioimpedance for body composition analysis. The second device, L-Dex U400 BIS [74]–[76], was specifically designed to estimate the amount of ECW. This device has been FDA cleared specifically for lymphedema use. The L-Dex uses the principles of segmental BIS, which involves passing a small alternating current of $200 \mu\text{A}$ at a frequency range of to 1000 kHz through the affected limb. The impedance measurements gathered with the L-Dex are inversely proportional to the amount of fluid [75]. The L-Dex provides information about an extracellular fluid ratio, known as L-Dex, which is known as a lymphedema index. Despite having been FDA cleared, there are limited studies using this device, so further research should be conducted to validate its reliability and ensure, not only that the data collected are accurate, but also that the device does not present the same type of issues that have been encountered using all methods related to bioimpedance.

4) Bioelectrical Impedance Analysis Vectors: Due to inconsistent results obtained when using bioelectrical impedance spectroscopy, other studies have aimed to use bioelectrical impedance vectors to assess changes in water content. For instance, Lukaski *et al.* performed a study to measure TBW using resistance (R) and reactance (Xc), in order to compare it to deuterium dilution data that were obtained from blood samples taken after each woman drank the dilution [77]. Standing height was standardized and plotted on a bivariate graph, which yielded a vector with direction and length [77]. This team of researchers concluded that the impedance vectors obtained were significantly correlated with the deuterium dilution assessment of TBW during and after pregnancy [77]. Additionally, the changes in the parameters were also related.

The majority of research studies conducted on bioelectrical impedance vectors have been limited to the measurements of TBW and its validation has been limited. Additionally, further studies should be conducted using this technique for estimating ECW content.

5) Additional Applications of Bioelectrical Impedance: Another application for bioelectrical impedance, not as widely known, is the measurement of skin blood flow (SBF) [78], [79]. A study conducted by the Naval Health Research Center in 1994 aimed to determine the effect of changes in SBF on bioelectrical resistance [80]. In order to alter the SBF of the subjects' right arm, where the electrodes were placed, the left arm of each of the 23 male individuals was

repeatedly submerged in water for 1 min and removed from it for 3 min, repeating this procedure three times for a total of 12 min [80]. This was done in room temperature at three different temperatures of water 5, 15, and $35 \text{ }^\circ\text{C}$.

In order to measure SBF, the researchers used laser-Doppler flowmeter and placed a probe on the right hand's second finger (dorsal side) of each participant. The laser-Doppler method consists of a helium-neon laser beam of low power that penetrates the skin, so the light that strikes and moves blood cells is reflected with a frequency shift, which allows determining an estimate of the relative blood flow [80].

The results obtained in this study suggest that the changes in resistance that were seen when the arm was immersed in cold water are caused, not only to the change in position, but also to the cold-induced vasoconstriction [80]. Although these results agree with those obtained by a previous study done in 1993, where Liang and Norris found an inverse correlation between the SBF and skin resistance during vasodilation induced by exercise [79], [80]. However, in order to obtain baseline measurements of the resistance, electrodes were placed on the index finger, but the values collected were 50% greater than those collected in the arm during the standard procedure. This may be explained by the smaller cross-sectional area of the finger when compared to the wrist [80]. Even though the resistance in the finger was not equivalent to the resistance in the arm, the results obtained demonstrate the relative alterations in resistance that comes along with vasoconstriction [80]. Finally, even though this study does not seem to be very accurate and precise due to the measurements of SBF and resistance being collected in different parts of the body, this study somehow proved that SBF and resistance are significantly and inversely related [80].

6) Electrode Size and Impedance Variations: When measuring skin impedance, surface electrodes are able to convert the ionic current that is found in the body into electronic current [81]–[83]. However, the reality is that the skin, tissue, electrodes, and amplifiers recording the signal limit the ability to reproduce the physiological signal with high fidelity [84]. Several studies have shown that performing dc measurements of skin-electrode impedance will not provide enough information. However, when using ac measurements, it is possible to obtain a more accurate estimate of skin-electrode impedance [81].

The junction between the electrode and the skin arises from the need of directing electrical currents into or away from the body. Electrodes are composed of several conductive elements, so when compared to the body, there is a small potential found at that physical interface between the skin and the electrode [82], [85]. In addition to that potential, there is also the junction's characteristic impedance, which is larger at lower frequencies than at higher frequencies.

It is widely known that the model of an electrode in the skin is given by a resistance that is connected in parallel with a series network composed of a resistance and capacitance, which represents the electrode/skin impedance [82], [85]. Application of low frequencies to this circuit model would result in a high-impedance value, while high frequencies would result in lower impedance.

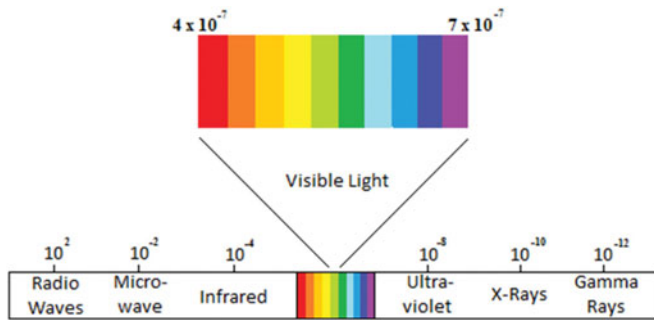


Fig. 6. Electromagnetic spectrum.

Additionally, the impedance level also depends on the size of the electrode. For instance, the impedance of the surface electrode/skin junction decreases when the electrode surface area is bigger. Similarly, when the surface area of the electrodes is small, then the impedance value would be much higher [82], [85]. Therefore, it is important to keep these factors in mind when designing electrodes for collecting measurements in the skin.

C. Optical Techniques

Light absorption via tissue spectroscopy provides a good estimate of the chemical composition of the tissue. Chromophores are the molecules capable of absorbing light and these can be divided in two major types depending on the type of absorption, electronic transitions, and vibrational transitions [86], [87].

Electronic transitions are relatively energetic and they are usually associated with absorption of UV, visible, and NIR wavelengths (see Fig. 6). Examples of these include chlorophyll, heme, carotenoids, and melanin, among others [88]. On the other hand, vibrational transitions include water, which is the most dominant chromophore in biology [88]. Infrared (IR) spectroscopy studies the bonds that can resonantly vibrate or twist in response to wavelength in the IR spectrum, and, hence, absorb such photons [88]. In IR spectroscopy, the strongest contributor to tissue absorption is water absorption.

A good understanding of the optical properties of the tissue is critical in predicting light distribution in biological tissue. The optical properties of tissue can be described based on the absorption coefficient (μ_a), the tissue real refractive index (n'), the scattering coefficient (μ_s), and the scattering function ($p(\theta, \psi)$, where θ is the scattering deflection angle and ψ is the scattering azimuthal angle) [89].

1) Perometry: Perometry is a technique where an IR optical electronic scanner is used to compute the volume of a body part, as shown in Fig. 7. Perometry has been verified to be accurate when compared to the gold standard of water displacement and a great tool lymphedema research [46]. Perometry works on the Archimedes principle [90], [91].

This technique can only be accurate if the affected body area is positioned consistently for every measurement. In addition, the system must also be calibrated for accuracy. This makes this system inconvenient for the patient not user friendly, requiring specialized personnel.

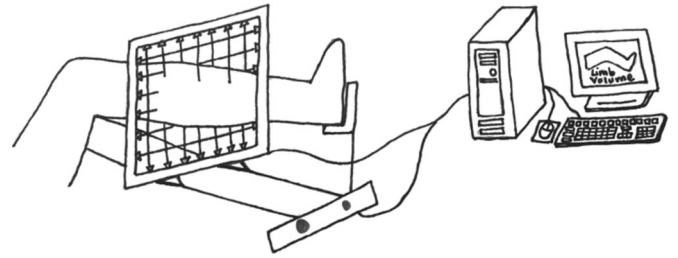


Fig. 7. IR optoelectronic system or perometer (adapted from [91], [92]).

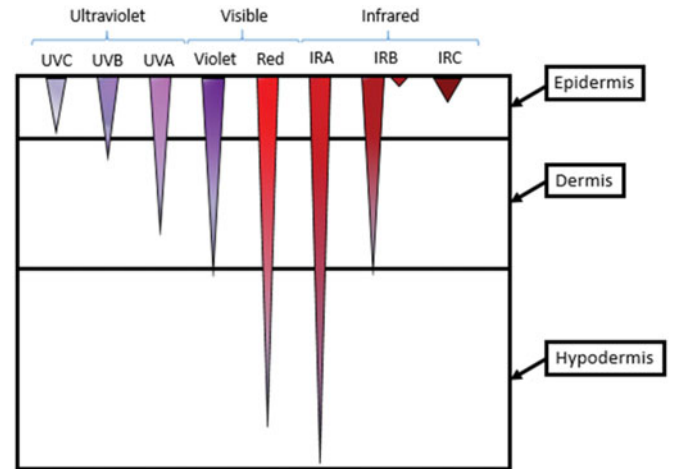


Fig. 8. Sample of how different types of light penetrate the skin (adapted from [94], [95]).

2) Optical Depth of Penetration and Separation Distance Between the Light Source and Optical Detector:

The penetration depth of light in tissue can be identified by the distance over which fluence rate drops to e^{-1} of its initial value and is given by

$$\delta = \frac{1}{\mu_{\text{eff}}} \quad (21)$$

where μ_{eff} is the effective attenuation coefficient for diffuse light [93].

The depth of optical penetration not only depends on the type of light used, but it will also depend directly on the separation distance between the light source and the optical detector. However, there are no studies related to whether the depth of penetration needed to encounter the subcutaneous layer, which is approximately 2.2 mm in the arm and 1.9 mm in the thigh [96], can actually be reached. This is why Monte-Carlo simulations of light transport can be performed, in order to understand light traveling through tissue and determine the maximum depth of optical penetration based on variations of the light source-optical detector separation distance, which commonly range from 0.8 to 3.0 mm as found in the literature [97]. Additionally, this depth will also depend on the wavelength use, since the IR and red visible wavelengths are able to penetrate deeper in the skin than wavelengths such as the violet visible or the ultraviolet as seen in Fig. 8 [94].

3) Medical Imaging: Medical imaging approaches, such as CT, MRI, and ultrasound are often used for lymphedema diagnosis [46]. CT imaging has shown to be highly sensitive and specific for lymphedema diagnosis [98]. MRI can provide a sensitive diagnosis of lymphedema with detailed soft-tissue architecture, without radiation exposure [99]. These techniques can provide accurate information about the presence excessive interstitial fluids when the information is compared with patient history, physical examination, and other imaging tests. However, these techniques are limited to the clinical lab set up and not convenient for continuous monitoring of lymphedema disease/treatment progression. Radio-labeled particles are injected under the area of the skin to be imaged during lymphoscintigraphy [46]. Due to radio-labeled-enhance imaging, this approach can provide accurate diagnosis of irregularities in lymphatic flows, lymph uptakes, and treatment response [23]. A detailed risk to benefit analysis is necessary before using nuclear dye for lymphedema imaging. With advances in optical imaging, a 3-D surface imaging approach can provide detailed information of the noncontact volume measurement with higher speed, accuracy, and ease of use [100].

D. Comparison of Techniques

1) Water Displacement and Perometry: In a research study conducted by Tierney *et al.*, perometry was compared to the standard approach of water displacement and two other indirect techniques to measure limb volume [91]. The method of perometry consists on having a limb pass through a plastic rigid frame with four sides, which allows the limb to be moved along a rail in the limb's long axis [91], [101]. The aforementioned frame contains a couple of arrays of IR emitting diodes located at right angles of one another and on the opposite side of these, there are a couple of arrays of IR detecting diodes, as seen in Fig. 7 [91]. The frame moves along the limb, which causes the IR beams to be interrupted, allowing the sensors to determine the dimensions of the limb electronically.

The other methods implemented in this study were water displacement, the disc model method, and the Frustrum method, which were all previously described. The disc model method consists on placing the patient's limb on a graduated device that has been marked at 3-cm intervals as reference points [91]. The limb can be then divided into 3-cm discs between these reference points in order to determine the circumference of each disc. Then, the volume can be calculated using the following formula:

$$\sum_{i=1}^n \left(\frac{C_i^2}{4\pi} \right) (h) \quad (22)$$

where C is the circumference of the disc and h is the height of the disc [91]. On the other hand, the Frustrum method consists on assuming that the limb has a shape that can be approximated to that of a truncated cone or frustrum [91]. This means that the volume of the limb can be calculated using the dimensions of the circumference at the lower and upper reference points, and

TABLE II
COMPARISON OF THE DIFFERENT LIMB VOLUME RESULTS OBTAINED FROM THE METHODS IMPLEMENTED BY TIERNEY IN VOLUNTEERS WITH NORMAL AND DISEASED LIMBS ADAPTED FROM [91]

Method	Normal limbs ml (s.d.)	Diseased limbs ml (s.d.)
Water displacement	1802 (268)	
Perometer	1809 (262)	2415 (995)
Disc method	1923 (306) [†]	2494 (969)
Frustrum method	1905 (372) [†]	2413 (870)

^{*} $p < 0.05$ versus water displacement.
[†] $p < 0.05$ versus water displacement (ANOVA, Fisher's least significant difference).

the distance between these with the following formula:

$$\left(\frac{\pi}{12\pi^2} \right) (h) (C^2 + Cc + c^2) \quad (23)$$

where C is the upper reference point, c is the lower reference point, and h is the distance between the two reference points [91].

Based on the results obtained from this study (see Table II), and after comparing the data gathered using the different methods, Tierney *et al.* concluded that perometry is a technique that provides much more accurate results than indirect traditional methods for measuring limb volume, and, therefore, it is a very useful tool for research and clinical applications.

2) Bioimpedance and Perometry: Moseley *et al.* [59] conducted a study to compare multifrequency bioimpedance analysis and perometry when measuring the effectiveness of a treatment in secondary leg lymphedema. This study provided a good correlation between perometry and MF-BIA; however, bioimpedance was found to provide a measure of intra and ECW, whereas perometry also measures changes in fibers, cells, and other components [59]. This suggests that BIA is more useful for measuring the actual fluid in the limb, whereas perometry measures the entire volume of the affected extremity.

Some of the drawbacks that were found for these techniques during this study include inconvenience. For instance, in the case of bioimpedance, the patient must stand upright for 2 entire min and must have intact limbs (no amputees) [59]. In this study, bioimpedance was used to measure changes in the whole body ECW, so even though it was cross correlated with perometry, the fact that the amount of total ECW was reduced may not necessarily be directly or indirectly related to the reduction of fluid accumulation in lymphedema. Since this technique measured whole body ECW, it is hard to draw conclusions on what is actually going on in the affected limb. Therefore, the method of bioimpedance should be further explored for localized measurement, in order to confirm its validity when estimating limb volume in patients with lymphedema.

IV. DISCUSSION AND CONCLUSION

In this study, lymphedema and current methods for its detection were discussed. Lymphedema is a condition characterized by excessive fluid accumulation in the subcutaneous tissue due to disruption of the lymphatic system. Throughout the years, different types of methodologies have been implemented to

measure lymphedema and estimate limb volume; however, there is still no method that allows continuous monitoring of the disease to better understand it.

Some of the most common methods for measuring lymphedema include measures of volumes, such as tape measurements and the gold standard of water displacement, electrical techniques, such as bioelectrical impedance analysis, and optical methods, such as optical spectroscopy and perometry. Some of the optical and electrical techniques can be used to measure both water content and the behavior of blood flow in the affected tissue. It is critical to know these two parameters because as the amount of fluid accumulated increases, the flow of blood may decrease due to blood vessel constriction that occurs as a result of increased pressure in the limb. Therefore, gathering these measurements is important in better understanding lymphedema as it progresses.

All measures of volume can be accurate up to a certain extent, when performed properly. These are most accurate when done in the legs and/or arms. Even though tape measurements were developed for the head and neck initially, they are not considered true volume measurements, and have not been standardized [46].

Bioelectrical impedance analysis has been used in different studies to measure water content, as shown in studies by Lukaski's [50], [55], [77], which is useful when estimating limb volume in patients with lymphedema. After carefully reviewing a large amount of research studies, it was possible to understand the advantages and disadvantages presented by the different variations of bioelectrical impedance techniques. Nevertheless, it seems that MF-BIA and BIS are the techniques that provide more reliability and accuracy when it comes to measuring ECW content, since both techniques allow researchers to gather measurements at low frequencies. These measurements can then be easily used with the mathematical formulas, as explained above, to calculate the amount of ECW. As these techniques have limited validation testing and they have only been used for measuring whole body ECW, further studies should be conducted, in order to estimate the localized amount of ECW that is found in the affected limb. In order to do this, a modified algorithm that only accounts for the parameters of the corresponding limb must be developed. Both MF-BIA and BIS should be further validated by gathering data from different types of population (i.e., different ethnicities, different ages, etc), as well as from unhealthy individuals. This would minimize the error when amounts of fluid are estimated.

On the other hand, optical spectroscopy has also been used to measure both of these parameters. For instance, Qassem and Kyriacou [102] measured water content using NIRS. Additionally, Stamatias *et al.* [103] conducted a study that aimed to measure induced edema in the skin using optical spectroscopy, where the author looked at both the amount of water and hemoglobin using the corresponding wavelengths of 970 nm for the former and 560–580 nm for the latter. Although these studies have shown that optical spectroscopy is useful for gathering surface measurements from the skin, no studies have been conducted using this method for measuring lymphedema. Therefore, since it is unknown whether a light emitter could reach the depth of fluid accumulation in the affected limb, it is important to con-

duct additional testing and validate the approach to determine whether it would be effective for providing useful information about lymphedema. Despite the lack of validation, it seems that NIRS could be a promising technique that would be able to provide key information about the hemodynamics of lymphedema, as the condition progresses.

Review of the present technologies leads us to the conclusion that there is a critical need of developing robust and quantitative approach for lymphedema monitoring. By combining electrical impedance and optical measurement, we can exploit the benefits of electrical and optical approaches. Ideally, a novel point-of-care device which patients can use to monitor lipedema progression and treatment efficiency without constant interference of the clinical personal can enhance the lymphedema disease management. However, further research in electrical and optical methods for measuring lymphedema must be conducted, in order to fully understand what may worsen the disease, as well as to learn about the evolution of the condition. Ultimately, the goal is to find a better way to treat and monitor the condition using an easier, more convenient, and more affordable approach, and maybe even find a way to prevent it and cure it, if possible.

ACKNOWLEDGMENT

The authors would like to thank the Florida Georgia Louis Stoke Alliance for Minority Participation program.

REFERENCES

- [1] K. A. Holbrook and G. F. Odland, "Regional differences in the thickness (cell layers) of the human stratum corneum: An ultrastructural analysis," *J. Investigative Dermatol.*, vol. 62, pp. 415–422, Apr. 1974.
- [2] E. McLafferty *et al.*, "The integumentary system: Anatomy, physiology and function of skin," *Nursing Stand*, vol. 27, pp. 35–42, Sep. 19–25, 2012.
- [3] *Layers of the Skin*. (2015, Oct. 1). [Online]. Available: <http://training.seer.cancer.gov/melanoma/anatomy/layers.html>
- [4] K. L. McCance and S. E. Huether, *Pathophysiology: The Biologic Basis For Disease in Adults and Children*. Amsterdam, The Netherlands: Elsevier, 2014.
- [5] A. G. Warren *et al.*, "Lymphedema: A comprehensive review," *Ann. Plastic Surg.*, vol. 59, pp. 464–472, Oct. 2007.
- [6] R. J. Maughan *et al.*, "Errors in the estimation of hydration status from changes in body mass," *J. Sports Sci.*, vol. 25, pp. 797–804, May 2007.
- [7] S. G. Rockson, "Lymphedema," *Amer. J. Med.*, vol. 110, pp. 288–295, Mar. 2001.
- [8] M. J. Davis *et al.*, "Determinants of valve gating in collecting lymphatic vessels from rat mesentery," *Amer. J. Physiol. Heart Circ. Physiol.*, vol. 301, pp. H48–H60, Jul. 2011.
- [9] M. Skobe and M. Detmar, "Structure, function, and molecular control of the skin lymphatic system," *J. Investigative Dermatol. Symp. Proc.*, vol. 5, pp. 14–19, Dec. 2000.
- [10] G. M. Dittami and R. D. Rabbitt, "Electrically evoking and electrochemically resolving quantal release on a microchip," *Lab Chip*, vol. 10, pp. 30–35, 2010.
- [11] M. A. Swartz, "The physiology of the lymphatic system," *Adv. Drug Del. Rev.*, vol. 50, pp. 3–20, Aug. 23, 2001.
- [12] A. B. Rossi and A. L. Vergnanini, "Cellulite: A review," *J. Eur. Acad. Dermatol. Venerol.*, vol. 14, pp. 251–262, Jul. 2000.
- [13] C. C. Yang and G. Cotsarelis, "Review of hair follicle dermal cells," *J. Dermatol. Sci.*, vol. 57, pp. 2–11, Jan. 2010.
- [14] M. T. De Sanctis *et al.*, "Treatment of edema and increased capillary filtration in venous hypertension with total triterpenic fraction of *Centella asiatica*: A clinical, prospective, placebo-controlled, randomized, dose-ranging trial," *Angiology*, vol. 52, suppl., 2, pp. S55–S59, Oct. 2001.
- [15] S. Baranoski and E. A. Ayello, *Wound Care Essentials: Practice Principles*. Baltimore, MD, USA: Lippincott Williams & Wilkins, 2008.

- [16] M. A. Fonder *et al.*, "Lipedema, a frequently unrecognized problem," *J. Amer. Acad. Dermatol.*, vol. 57, pp. S1–S3, Aug. 2007.
- [17] C. J. R. Stewart *et al.*, "Acquired lymphangiectasia ('lymphangioma circumscriptum') of the vulva: A report of eight cases," *Pathology*, vol. 41, pp. 448–453, 2009.
- [18] R. M. Bhat *et al.*, "Cutaneous lymphangiectasia of the vulva secondary to tuberculosis," *Indian J. Sexually Transmitted Dis.*, vol. 33, pp. 35–37, Jan. 2012.
- [19] M. Flour, "Dermatological issues in lymphoedema and chronic oedema," *Int. Lymphoedema Framework*, vol. 27, pp. 49–56, 2013.
- [20] W. L. Olszewski *et al.*, "Where do lymph and tissue fluid accumulate in lymphedema of the lower limbs caused by obliteration of lymphatic collectors?" *Lymphology*, vol. 42, pp. 105–111, Sep. 2009.
- [21] P. Chen *et al.*, "Amperometric detection of quantal catecholamine secretion from individual cells on micromachined silicon chips," *Anal. Chem.*, vol. 75, pp. 518–524, Feb. 1, 2003.
- [22] E. Daniel-Spiegel *et al.*, "Hydrops fetalis: An unusual prenatal presentation of hereditary congenital lymphedema," *Prenatal Diagn.*, vol. 25, pp. 1015–1018, Nov. 2005.
- [23] C. Bellini *et al.*, "Lymphatic dysplasias in newborns and children: The role of lymphoscintigraphy," *J. Pediatr.*, vol. 152, pp. 587–589, Apr. 2008.
- [24] A. K. Greene and C. C. Schook, "Primary lymphedema: Definition of onset based on developmental age," *Plastic Reconstr. Surg.*, vol. 129, pp. 221e–222e, Jan. 2012.
- [25] J. M. Lewis and E. R. Wald, "Lymphedema praecox," *J. Pediatr.*, vol. 104, pp. 641–648, May 1984.
- [26] C. Rizzo *et al.*, "Lymphedema praecox," *Dermatol. Online J.*, vol. 15, pp. 1–4, 2009.
- [27] G. Murdaca *et al.*, "Current views on diagnostic approach and treatment of lymphedema," *Amer. J. Med.*, vol. 125, pp. 134–140, Feb. 2012.
- [28] E. S. Wheeler *et al.*, "Familial lymphedema praecox: Meigs' disease," *Plastic Reconstr. Surg.*, vol. 67, pp. 362–364, Mar. 1981.
- [29] R. G. Baumeister *et al.*, "Experimental basis and first application of clinical lymph vessel transplantation of secondary lymphedema," *World J. Surg.*, vol. 5, pp. 401–407, May 1981.
- [30] J. Deng *et al.*, "Prevalence of secondary lymphedema in patients with head and neck cancer," *J. Pain Symptom Manage.*, vol. 43, pp. 244–252, Feb. 2012.
- [31] A. Zimmermann *et al.*, "Efficacy of manual lymphatic drainage in preventing secondary lymphedema after breast cancer surgery," *Lymphology*, vol. 45, pp. 103–112, Sep. 2012.
- [32] C. Miaskowski *et al.*, "Lymphatic and angiogenic candidate genes predict the development of secondary lymphedema following breast cancer surgery," *Plos One*, vol. 8, p. e60164, 2013.
- [33] D. N. Finegold *et al.*, "Connexin 47 mutations increase risk for secondary lymphedema following breast cancer treatment," *Clin. Cancer Res.*, vol. 18, pp. 2382–2390, Apr. 15, 2012.
- [34] T. DiSipio *et al.*, "Incidence of unilateral arm lymphoedema after breast cancer: A systematic review and meta-analysis," *Lancet Oncol.*, vol. 14, pp. 500–515, May 2013.
- [35] K. Togawa *et al.*, "Risk factors for self-reported arm lymphedema among female breast cancer survivors: A prospective cohort study," *Breast Cancer Res.*, vol. 16, pp. 1–15, 2014.
- [36] S. L. Showalter *et al.*, "Lifestyle risk factors associated with arm swelling among women with breast cancer," *Ann. Surg. Oncol.*, vol. 20, pp. 842–849, Mar. 2013.
- [37] M. Oremus *et al.*, "Systematic review: Conservative treatments for secondary lymphedema," *BMC Cancer*, vol. 12, p. 6, 2012.
- [38] L. M. Zeldenryk *et al.*, "The emerging story of disability associated with lymphatic filariasis: A critical review," *PLoS Neglected Trop. Dis.*, vol. 5, p. e1366, Dec. 2011.
- [39] N. H. Cox, "Oedema as a risk factor for multiple episodes of cellulitis/erysipelas of the lower leg: A series with community follow-up," *Brit. J. Dermatol.*, vol. 155, pp. 947–950, Nov. 2006.
- [40] P. C. Woo *et al.*, "Cellulitis complicating lymphoedema," *Eur. J. Clin. Microbiol. Infectious Dis.*, vol. 19, pp. 294–297, Apr. 2000.
- [41] J. A. Carlson, "Lymphedema and subclinical lymphostasis (microlymphedema) facilitate cutaneous infection, inflammatory dermatoses, and neoplasia: A locus minoris resistentiae," *Clin. Dermatol.*, vol. 32, pp. 599–615, Sep./Oct. 2014.
- [42] Lymphatic Education and Research Network. (2015, Oct. 1). [Online]. Available: <http://lymphaticnetwork.org/living-with-lymphedema/lymphedema-and-lymphatic-diseases-affect-millions-and-concern-us-all>
- [43] A. Sagen *et al.*, "Validity for the simplified water displacement instrument to measure arm lymphedema as a result of breast cancer surgery," *Arch. Phys. Med. Rehabil.*, vol. 90, pp. 803–809, May 2009.
- [44] B. J. Smoot *et al.*, "Comparison of diagnostic accuracy of clinical measures of breast cancer-related lymphedema: Area under the curve," *Arch. Phys. Med. Rehabil.*, vol. 92, pp. 603–610, Apr. 2011.
- [45] R. S. Meijer *et al.*, "Validity and intra- and interobserver reliability of an indirect volume measurements in patients with upper extremity lymphedema," *Lymphology*, vol. 37, pp. 127–133, Sep. 2004.
- [46] Position Statement of the National Lymphedema Network. (2015, Oct. 1). [Online]. Available: <http://www.lymphnet.org/pdfDocs/nltreatment.pdf>
- [47] M. Oremus *et al.*, Diagnosis and treatment of secondary lymphedema, May 28, 2010.
- [48] A. P. Sander *et al.*, "Upper-extremity volume measurements in women with lymphedema: A comparison of measurements obtained via water displacement with geometrically determined volume," *Phys. Ther.*, vol. 82, pp. 1201–1212, Dec. 2002.
- [49] M. Piccolino, "Luigi galvani and animal electricity: Two centuries after the foundation of electrophysiology," *Trends Neurosci.*, vol. 20, pp. 443–448, Oct. 1997.
- [50] H. C. Lukaski, "Methods for the assessment of human body composition: Traditional and new," *Amer. J. Clin. Nutr.*, vol. 46, pp. 537–556, Oct. 1987.
- [51] S. F. Khalil *et al.*, "The theory and fundamentals of bioimpedance analysis in clinical status monitoring and diagnosis of diseases," *Sens., Basel*, vol. 14, pp. 10895–10928, 2014.
- [52] U. G. Kyle *et al.*, "Bioelectrical impedance analysis—Part I: Review of principles and methods," *Clin. Nutr.*, vol. 23, pp. 1226–1243, Oct. 2004.
- [53] P. L. Cox-Reijven and P. B. Soeters, "Validation of bio-impedance spectroscopy: Effects of degree of obesity and ways of calculating volumes from measured resistance values," *Int. J. Obesity Relat. Metab. Disord.*, vol. 24, pp. 271–80, Mar. 2000.
- [54] T. Tzotzas *et al.*, "Body composition analysis using radionuclides," in *Handbook of Anthropometry*, V. R. Preedy, Ed. New York, NY, USA: Springer, 2012, pp. 185–203.
- [55] H. C. Lukaski and W. W. Bolonchuk, "Estimation of body-fluid volumes using tetrapolar bioelectrical impedance measurements," *Avia. Space Environ. Med.*, vol. 59, pp. 1163–1169, Dec. 1988.
- [56] D. J. Casa *et al.*, "National athletic trainers' association position statement: Fluid replacement for athletes," *J. Athletic Training*, vol. 35, pp. 212–224, Apr. 2000.
- [57] T. G. Lohman, "Skinfolds and body density and their relation to body fatness—A review," *Hum. Biol.*, vol. 53, pp. 181–225, 1981.
- [58] A. DeLorenzo, A. Andreoli, J. Matthie, and P. Withers, "Predicting body cell mass with bioimpedance by using theoretical methods: A technological review," *J. Appl. Physiol.*, vol. 82, pp. 1542–1558, May 1997.
- [59] A. Moseley *et al.*, "Combined opto-electronic perometry and bioimpedance to measure objectively the effectiveness of a new treatment intervention for chronic secondary leg lymphedema," *Lymphology*, vol. 35, pp. 136–143, 2002.
- [60] R. F. Kushner and D. A. Schoeller, "Estimation of total body water by bioelectrical impedance analysis," *Amer. J. Clin. Nutr.*, vol. 44, pp. 417–424, Sep. 1986.
- [61] G. Sergi *et al.*, "Accuracy of bioelectrical impedance analysis in estimation of extracellular space in healthy subjects and in fluid retention states," *Ann. Nutr. Metab.*, vol. 38, pp. 158–165, 1994.
- [62] D. H. Kim *et al.*, "Epidermal electronics," *Science*, vol. 333, pp. 838–843, Aug. 12, 2011.
- [63] D. H. Kim *et al.*, "Flexible and stretchable electronics for biointegrated devices," *Annu. Rev. Biomed. Eng.*, vol. 14, pp. 113–128, 2012.
- [64] K. J. Shafer *et al.*, "Validity of segmental multiple-frequency bioelectrical impedance analysis to estimate body composition of adults across a range of body mass indexes," *Nutrition*, vol. 25, pp. 25–32, Jan. 2009.
- [65] U. G. Kyle *et al.*, "Bioelectrical impedance analysis—Part II: Utilization in clinical practice," *Clin. Nutr.*, vol. 23, pp. 1430–1453, 2004.
- [66] X. Huang *et al.*, "Epidermal differential impedance sensor for conformal skin hydration monitoring," *Biointerphases*, vol. 7, p. 1–9, Dec. 2012.
- [67] S. Demura *et al.*, "Percentage of total body fat as estimated by three automatic bioelectrical impedance analyzers," *J. Physiol. Anthropol. Appl. Hum. Sci.*, vol. 23, pp. 93–99, 2004.
- [68] P. Deurenberg *et al.*, "Multi-frequency impedance for the prediction of extracellular water and total body water," *Brit. J. Nutr.*, vol. 73, pp. 349–358, Mar. 1995.

- [69] G. P. Pichler *et al.*, "A critical analysis of whole body bioimpedance spectroscopy (BIS) for the estimation of body compartments in health and disease," *Med. Eng. Phys.*, vol. 35, pp. 616–625, May 2013.
- [70] B. A. Shanholtzer and S. A. Patterson, "Use of bioelectrical impedance in hydration status assessment: Reliability of a new tool in psychophysiology research," *Int. J. Psychophysiol.*, vol. 49, pp. 217–226, Sep. 2003.
- [71] S. M. Shirreffs, "Markers of hydration status," *J. Sports Med. Phys. Fitness*, vol. 40, pp. 80–84, Mar. 2000.
- [72] T. Hanai, "Dielectric theory on the interfacial polarization for two-phase," *Bull. Inst. Chem. Res.*, vol. 39, pp. 341–367, 1962.
- [73] M. Y. Jaffrin and H. Morel, "Body fluid volumes measurements by impedance: A review of bioimpedance spectroscopy (BIS) and bioimpedance analysis (BIA) methods," *Med. Eng. Phys.*, vol. 30, pp. 1257–1269, Dec. 2008.
- [74] M. Van Loan *et al.*, "Use of bioimpedance spectroscopy to determine extracellular fluid, intracellular fluid, total body water, and fat-free mass," in *Human Body Composition*, vol. 60, K. Ellis and J. Eastman, Eds. New York, NY, USA: Springer, 1993, pp. 67–70.
- [75] J. E. Bae *et al.*, "The effect of static magnetic fields on the aggregation and cytotoxicity of magnetic nanoparticles," *Biomaterials*, vol. 32, pp. 9401–9414, Dec. 2011.
- [76] M. R. Fu *et al.*, "L-dex ratio in detecting breast cancer-related lymphedema: Reliability, sensitivity, and specificity," *Lymphology*, vol. 46, pp. 85–96, Jun. 2013.
- [77] H. C. Lukaski *et al.*, "Assessment of change in hydration in women during pregnancy and postpartum with bioelectrical impedance vectors," *Nutrition*, vol. 23, pp. 543–550, Jul./Aug. 2007.
- [78] M. T. Liang *et al.*, "Skin temperature and skin blood flow affect bioelectric impedance study of female fat-free mass," *Med. Sci. Sports Exerc.*, vol. 32, pp. 221–227, Jan. 2000.
- [79] M. T. Liang and S. Norris, "Effects of skin blood flow and temperature on bioelectric impedance after exercise," *Med. Sci. Sports Exerc.*, vol. 25, pp. 1231–1239, Nov. 1993.
- [80] M. B. Beckett, J. A. Hodgdon, W. Woods, and B. W. Appleton, "Skin blood flow and bioelectrical impedance," Naval Health Res. Center, San Diego, CA, USA, DTIC Document Rep. 94-17, 1994.
- [81] A. B. C. Assambo, R. Dozio, and M. J. Burke, "Determination of the parameters of the skin-electrode impedance model for ECG measurement," in *Proc 6th Int. Conf. Electron., Hardw., Wireless Opt. Commun., Communications*, Corfu Island, Greece, 16–19 Feb. 2007, pp. 90–95.
- [82] S. Lee and J. Kruse, "Biopotential electrode sensors in ECG/EEG/EMG systems," *Analog Devices*, vol. 200, pp. 1–2, 2008.
- [83] A. V. Delgado *et al.*, "Measurement and interpretation of electrokinetic phenomena," *J. Colloid Interface Sci.*, vol. 309, pp. 194–224, May 15, 2007.
- [84] S. R. Wiese *et al.*, "Electrocardiographic motion artifact versus electrode impedance," *IEEE Trans Biomed Eng.*, vol. 52, no. 1, pp. 136–139, Jan. 2005.
- [85] T. Keller and A. Kuhn, "Electrodes for transcutaneous (surface) electrical stimulation," *J. Autom. Control*, vol. 18, pp. 35–45, 2008.
- [86] W. M. Zhang *et al.*, "Multidimensional femtosecond correlation spectroscopies of electronic and vibrational excitons," *J. Chem. Phys.*, vol. 110, pp. 5011–5028, Mar. 15, 1999.
- [87] S. Mukamel and D. Abramavicius, "Many-body approaches for simulating coherent nonlinear spectroscopies of electronic and vibrational excitons," *Chem. Rev.*, vol. 104, pp. 2073–2098, Apr. 2004.
- [88] M. Y. Berezin and S. Achilefu, "Fluorescence lifetime measurements and biological imaging," *Chem. Rev.*, vol. 110, pp. 2641–2684, May 12, 2010.
- [89] S. L. Jacques, "Optical properties of biological tissues: A review," *Phys. Med. Biol.*, vol. 58, pp. R37–R61, Jun. 7, 2013.
- [90] A. J. Spillane *et al.*, "Defining lower limb lymphedema after inguinal or ilio-inguinal dissection in patients with melanoma using classification and regression tree analysis," *Ann. Surg.*, vol. 248, pp. 286–293, Aug. 2008.
- [91] S. Tierney *et al.*, "Infrared optoelectronic volumetry, the ideal way to measure limb volume," *Eur. J. Vasc. Endovasc. Surg.*, vol. 12, pp. 412–417, Nov. 1996.
- [92] K. H. Labs *et al.*, "The reliability of leg circumference assessment: A comparison of spring tape measurements and optoelectronic volumetry," *Vasc. Med.*, vol. 5, pp. 69–74, 2000.
- [93] R. Splinter and B. A. Hooper, *An Introduction to Biomedical Optics*. New York, NY, USA: Taylor & Francis, 2006.
- [94] Scientific Committee on Emerging and Newly Identified Health Risks, "Health effects of artificial light," in *Proc. SCENIR, 17th Plenary Meeting*, 19 Mar. 2012, pp. 1–118.
- [95] L. Fodor *et al.*, "Light tissue interactions," in *Aesthetic Applications of Intense Pulsed Light*. New York, NY, USA: Springer, 2011, pp. 11–20.
- [96] M. Shimada *et al.*, "Melanin and blood concentration in human skin studied by multiple regression analysis: Experiments," *Phys. Med. Biol.*, vol. 46, pp. 2385–2395, Sep. 2001.
- [97] J. M. Schmitt *et al.*, "New methods for whole blood oximetry," *Ann. Biomed. Eng.*, vol. 14, pp. 35–52, 1986.
- [98] E. D. Monnin-Delhom *et al.*, "High resolution unenhanced computed tomography in patients with swollen legs," *Lymphology*, vol. 35, pp. 121–128, Sep. 2002.
- [99] T. C. Case *et al.*, "Magnetic resonance imaging in human lymphedema: Comparison with lymphangioscintigraphy," *Magn. Reson. Imag.*, vol. 10, pp. 549–558, 1992.
- [100] J. Geng, "Structured-light 3D surface imaging: A tutorial," *Adv. Opt. Photon.*, vol. 3, pp. 128–160, 2011.
- [101] S. A. Czerniec *et al.*, "Segmental measurement of breast cancer-related arm lymphoedema using perometry and bioimpedance spectroscopy," *Supportive Care Cancer*, vol. 19, pp. 703–710, May 2011.
- [102] M. Qassem and P. Kyriacou, "Comparing the rates of absorption and weight loss during a desorption test using near infrared spectroscopy," *Skin Res. Technol.*, vol. 19, pp. 137–144, 2013.
- [103] G. N. Stamatias *et al.*, "In vivo monitoring of cutaneous edema using spectral imaging in the visible and near infrared," *J. Investigative Dermatol.*, vol. 126, pp. 1753–1760, 2006.

Authors' photographs and biographies not available at the time of publication.